



A nonlinear friction compensation method using adaptive control and its practical application to an in-parallel actuated 6-DOF manipulator

Jee-Hwan Ryu^a, Jinil Song^b, Dong-Soo Kwon^{a,*}

^aDepartment of Mechanical Engineering, Korea Advanced Institute of Science and Technology, ME 3042 Taejon, South Korea

^bDepartment of Automation and Design Engineering, Korea Advanced Institute of Science and Technology, Seoul, South Korea

Received 15 October 1999; accepted 9 June 2000

Abstract

This paper presents a simple and effective nonlinear friction compensation method which is derived from an adaptive control strategy and its practical application to a linear actuator. The proposed adaptive friction compensation method is shown to be equivalent to the reversed integral controller that is easily applied to the conventional PID controller. The reversed integral controller reverses the sign of the integrator output as the sign of the velocity changes. It analyzes how the reversed control action can compensate for friction. The effectiveness of this approach is demonstrated by experiments on a 3-PRPS (Prismatic-Revolute-Prismatic-Spherical joints) in-parallel 6-DOF manipulator. © 2001 Published by Elsevier Science Ltd. All rights reserved.

Keywords: Nonlinear friction; Friction compensation; Adaptive control; Reversed integral control; Parallel manipulator

1. Introduction

In servo systems, steady-state errors and tracking errors are mainly caused by static friction (stiction), which depends on the velocity's direction, and the viscous friction that increases the damping of a system. The main way to remedy friction is to formulate a nonlinear friction model, identify its parameters, and suggest compensation algorithms.

Friction models have been widely studied by numerous researchers (Armstrong-Helouvry, 1993; Canudas de Wit, Astrom & Lischinsky, 1995; Canudas de Wit, Olsson, Astrom & Lischinsky, 1993). Friction is commonly modeled as a linear combination of Coulomb friction, stiction, viscous friction, and the Stribeck effect. However, the modeling of exact friction characteristics is not easy because friction characteristics are sensitive to various environmental factors: variations of the load, temperature, lubrication, and the assembly status of machines. A wide range of friction compensation

schemes have been proposed (Armstrong-Helouvry, Dupont & Canudas de Wit, 1994). Traditional PD controllers will not achieve satisfactory results because of steady-state errors. Even though the errors may be reduced using a high-gain PD controller (Wu & Paul, 1980), the high gain controller can cause system instability. The integrator of a PID controller can compensate for steady-state errors, but this will cause the generation of a limit cycle due to the fact that stick-slip friction is time-varying (Radcliffe & Southward, 1990; Townsend & Salisbury, 1987). As a model reference feed-forward method, adaptive schemes (Ge, Lee & Harris, 1998; Lewis, Jagannathan & Yesildirek, 1998; Polycarpou & Ioannou, 1993) have been proposed to compensate for nonlinear friction in a variety of mechanisms (Canudas de Wit, Astrom & Braun, 1987; Canudas de Wit, Noel, Auban & Broglianto, 1991), but these are usually based on certain linearized models or models with linearized parameters that are approximations of the nonlinear phenomenon. To strengthen the compensation of nonlinear friction, a new adaptive scheme was developed recently (Canudas de Wit & Ge, 1997), based on a new friction model (Canudas de Wit et al., 1995). Since the model reference feed-forward compensation depends on the friction model, the model error of friction can induce

* Corresponding author. Tel.: + 82-42-869-3042; fax: + 82-42-869-3210.

E-mail address: kwonds@me.kaist.ac.kr (D.-S. Kwon).

large tracking errors. To avoid using a friction model, a disturbance observer has been applied to compensate for friction (Ohnishi, Matsui & Hori, 1994; Ohnishi, Shiata & Murakami, 1996; Umeno & Hori, 1991). A disturbance observer based on friction compensation, which regards the bounded nonlinear friction terms as disturbances, does not need a friction model. However, due to the limited bandwidth of the disturbance observer, friction estimation errors usually yield tracking errors. To increase position accuracy and smoothness of motion, a smooth robust nonlinear controller is proposed for robot manipulators with joint stick-slip friction (Cai & Song, 1994, 1993).

This paper proposes a simple but effective nonlinear friction-compensation technique for the tracking of the 6-DOF 3PRPS parallel manipulator with unknown friction. The proposed method, which does not need a friction model, uses the integrator information of the PID feedback controller. It is well known that integral action in the feedback controller can remove the steady-state errors caused by constant disturbances. However, because of the hard nonlinear nature of stiction, it is difficult to compensate for stiction effectively with conventional integral control action. Circular motion of the developed parallel manipulator, for instance, stiction causes large tracking errors to appear at 60° intervals around the circle. If there is no disturbance when the motion direction changes, it can be assumed that the steady-state error is approximately zero. If there is stiction, non-zero values of the integrator exist. When the motion command is reversed and stiction exists, the sign of integrator output does not change immediately because of the accumulated errors. Therefore, the integrator output degrades tracking performance. To overcome this problem, this paper proposes a nonlinear friction-compensation method based on adaptive control (Slotine & Li, 1987, 1991) and its practical application. The proposed controller reverses the sign of the integrator output when the sign of the velocity changes (Song, Choi, Shim, Kwon & Cho, 1998). The method has been applied to the control of a 3-PRPS in-parallel manipulator, designed for micro positioning and excellent results have been obtained.

The remainder of this paper is organized as follows: Section 2 proposes a nonlinear friction compensation technique using an adaptive control strategy. Section 3 demonstrates the fact that the proposed controller is equivalent to the controller that reverses the sign of integrator output as the sign of velocity changes. Section 4 describes the reason why the reversed integral action can compensate for friction. In Section 5, the in-parallel 3PRPS (Prismatic-Revolute-Prismatic-Spherical joints) manipulator is described. Section 6 provides experimental results to illustrate the performances of the developed scheme. Finally, conclusions are presented in Section 7.

2. Proposed nonlinear friction compensation method

In this section, a nonlinear friction compensation method is proposed using an adaptive control strategy.

If Coulomb friction exists in the link of the parallel manipulator, and the damping term can be ignored, the dynamic equation of the link is as follows:

$$m\ddot{x} = u - \delta \operatorname{sgn}(\dot{x}). \quad (1)$$

To control the position of the parallel manipulator x , to track a desired trajectory x_d , and to identify the magnitude of Coulomb friction, adaptive control schemes are utilized. The control law is taken to be

$$u = \hat{m}\ddot{x}_r + K_D\dot{\varphi} + \hat{\delta} \operatorname{sgn}(\dot{x}), \quad (2)$$

where $\ddot{x}_r = \ddot{x}_d + \Lambda\dot{e}$, $\dot{x}_r = \dot{x}_d + \Lambda e$, $e = x_d - x$, $\varphi = \dot{x}_r - \dot{x}$, $K_D > 0$, $\Lambda > 0$ and \hat{m} , $\hat{\delta}$ are estimated values of m and δ , respectively.

If the estimated mass value of the moving part of the actuator \hat{m} is equivalent to m , the closed-loop error dynamic equation is formulated as follows:

$$m\dot{\varphi} = -K_D\varphi + \tilde{\delta} \operatorname{sgn}(\dot{x}), \quad (3)$$

where $\tilde{\delta} = \delta - \hat{\delta}$.

Consider a Lyapunov function candidate

$$V(t) = \frac{m\varphi^2}{2} + \frac{\tilde{\delta}^2}{2\Gamma}, \quad (4)$$

where Γ is a positive definite scalar. Then, the derivative of the Lyapunov function candidate is computed as

$$\begin{aligned} \dot{V}(t) &= m\varphi\dot{\varphi} + \tilde{\delta}\dot{\tilde{\delta}}/\Gamma \\ &= \varphi(-K_D\varphi + \tilde{\delta} \operatorname{sgn}(\dot{x})) + \tilde{\delta}\dot{\tilde{\delta}}/\Gamma \\ &= -K_D\varphi^2 + \tilde{\delta}(\varphi \operatorname{sgn}(\dot{x}) + \dot{\tilde{\delta}}/\Gamma). \end{aligned} \quad (5)$$

The derivative of the Lyapunov function candidate satisfies the condition,

$$\dot{V}(t) = -K_D\varphi^2 \leq 0 \quad (6)$$

by choosing the adaptation law to be

$$\dot{\tilde{\delta}} = -\Gamma\varphi \operatorname{sgn}(\dot{x}). \quad (7)$$

Since this implies that $V(t) \leq V(0)$, φ and $\tilde{\delta}$ are bounded. However, it is not sufficient to conclude that φ converges to zero because the dynamics are non-autonomous.

Check the uniform continuity of \dot{V} . The derivative of \dot{V} is

$$\ddot{V}(t) = \frac{2K_D}{m}\varphi^2 - 2K_D \operatorname{sgn}(\dot{x})\tilde{\delta}\dot{\varphi}.$$

This shows that \dot{V} is bounded because $\text{sgn}(\dot{x})$ is bounded and φ and $\hat{\delta}$ are shown above to be bounded. Hence, \dot{V} is uniformly continuous. The application of Barbalat's lemma (Slotine & Li, 1991) then indicates that φ converge to zero as time goes to infinity. Since φ and e are related as a stable first-order differential equation in e , the tracking error e and its derivative \dot{e} converge to zero as time goes to infinity. Note that, although φ converges to zero, the system is not asymptotically stable because $\hat{\delta}$ is only guaranteed to be bounded.

If the magnitude of Coulomb friction can be assumed to be constant or to vary quite slowly, the condition $\dot{\hat{\delta}} = -\hat{\delta}$ is satisfied. Thus, the Eq. (7) can be expressed as follows:

$$\dot{\hat{\delta}} = \Gamma \varphi \text{sgn}(\dot{x}). \quad (8)$$

Finally, the proposed control law is as follows:

$$u = \hat{m}\ddot{\theta}_r + K_D\varphi + \Gamma \text{sgn}(\dot{x}) \int_0^t \varphi \text{sgn}(\dot{x}) d\tau. \quad (9)$$

If the adaptive control law (9) is used, the tracking error e and its derivative \dot{e} converge to zero by compensating for Coulomb friction.

3. Control law synthesis for a practical application

This section presents a practical application method that implements the proposed nonlinear control law of Section 2.

The control input (9) is expanded as follows:

$$\begin{aligned} u &= \hat{m}\ddot{x}_r + K_D(\dot{e} + \Lambda e) + \Gamma \text{sgn}(\dot{x}) \int_0^t (\dot{e} + \Lambda e) \cdot \text{sgn}(\dot{x}) d\tau \\ &= \hat{m}\ddot{x}_r + K_P e + K_D \dot{e} + K_I \text{sgn}(\dot{x}) \int_0^t e \text{sgn}(\dot{x}) d\tau \\ &\quad + \Gamma \text{sgn}(\dot{x}) \int_0^t \dot{e} \text{sgn}(\dot{x}) d\tau. \end{aligned} \quad (10)$$

where $K_P = K_D\Lambda$ and $K_I = \Gamma\Lambda$. If the velocity direction is not changing, the control input (10) is composed of the inertia feed-forward term, the position of PID control, and the velocity I control. For a practical application, the feed-forward term has not been used as the control input.

This section will now analyze the nonlinear control input of (10) focusing on the action of the I -control. The nonlinear control input u_{Irev} is defined as follows:

$$u_{Irev} = K_I \text{sgn}(\dot{x}(t)) \int_0^t e \text{sgn}(\dot{x}(\tau)) d\tau. \quad (11)$$

This nonlinear input can be expanded as the velocity sign changes:

$$u_{Irev}(t) = \begin{cases} K_I \int_0^t e(\tau) d\tau, & 0 \leq t < t_1 \\ K_I \int_{t_1}^t e(\tau) d\tau - K_I \int_0^{t_1} e(\tau) d\tau & t_1 \leq t < t_2, \\ K_I \int_{t_2}^t e(\tau) d\tau - K_I \int_{t_1}^{t_2} e(\tau) d\tau + K_I \int_0^{t_1} e(\tau) d\tau & t_2 \leq t < t_3, \\ \vdots & \vdots \end{cases} \quad (12)$$

where $t_i (i = 1, 2, \dots)$ is the time when the velocity sign changes. This expanded result can explain the implicit meaning of the nonlinear control input u_{Irev} . The sign of the integrated output is reversed when the sign of the velocity changes and the integral control is continued from the instant when the velocity sign changes. The nonlinear control action is presented in a discrete domain:

$$I_{out}(k) = \begin{cases} I_{out}(k-1) + e(k) & \text{if } \dot{x}(k)\dot{x}(k-1) \geq 0, \\ -I_{out}(k-1) + e(k) & \text{if } \dot{x}(k)\dot{x}(k-1) < 0, \end{cases} \quad (13)$$

$$u_{Irev}(k) = K_I I_{out}(k), \quad (14)$$

where I_{out} is an integrated output. When the velocity sign changes, the sign of the integrator output is reversed. Therefore, the meaning of the reversed integrator output can be described as follows:

$$u_{Irev} = K_I \sum_{k=n} e(k) - K_I I_{out}(n-1), \quad (15)$$

where n is the instant when the velocity sign changes. The reversed integrator output acts to resist friction, and the integral controller restarts from the moment when the velocity sign changes ($k = n$).

The meaning of the integrated velocity error terms of the control input (the last term of Eq. (10)) can be explained in the above manner. However, the velocity error integration indicates position error. If the system bandwidth can be assumed to be higher than the desired command frequency range, the position error can be assumed to be almost zero at the instant just before the sign change of the velocity occurs by the position error integral control, even though the system has constant disturbances. Thus, the velocity error integrated nonlinear control action in (10) gives only a position P controller effect.

Finally, the proposed control law is summarized as follows:

$$\begin{aligned} u &= (K_P + \Gamma)e + K_D \dot{e} + u_{Irev} \\ &= (K_P + \Gamma)e + K_D \dot{e} + K_I \int_0^t e(\tau) d\tau + u_{FF}, \end{aligned} \quad (16)$$

where $u_{FF} = u_{Irev} - K_I \int_0^t e(\tau) d\tau$.

This control law is composed of a position PD controller and the reversed position error integral controller. The reversed position-error integral controller can be decomposed into a nominal integral controller and a feed-forward controller. The feed-forward control term is an additional control input to compensate for friction.

4. Reversed integral control action

This section explains the reason why the reversed integral control is so effective for friction compensation.

It is well known that an integral action in the feedback controller reduces steady-state errors due to constant disturbances. The integral action can compensate for Coulomb friction, which is the dc-components of the total friction force, and for viscous friction to some degree. In Fig. 1, which shows a proposed control structure, the position error is described as follows:

$$E(s) = \frac{(ms^3 + bs^2)x_d(s) + sT_i(s)}{ms^3 + (b + K_t K_D)s^2 + K_t K_P s + K_t K_I} \quad (17)$$

where s is the Laplace operator, K_t is the torque constant, $x_d(s)$ is the joint position command and $T_i(s)$ is the disturbance force. Note that the proposed control structure is the same as the conventional PID controller when there are no changes to the velocity sign.

The integrator output in the position servo loop is as follows:

$$u_I(s) = \frac{K_I}{s} E(s) = \frac{K_I(ms^2 + bs)x_d(s) + K_I T_i(s)}{ms^3 + (b + K_t K_D)s^2 + K_t K_P s + K_t K_I} \quad (18)$$

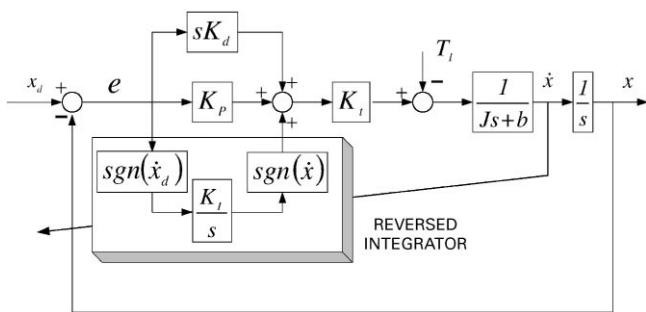


Fig. 1. Proposed controller structure.

Table 1
Steady-state error of position error and integrator output according to the position command and disturbance

Position command $x_d(s)$	Disturbance $T_i(s)$	Steady-state error E_{ss}	Integrator output at steady-state: $u_{I,ss}$
Step, sinusoidal	T_{const}/S	0	T_{const}/K_t

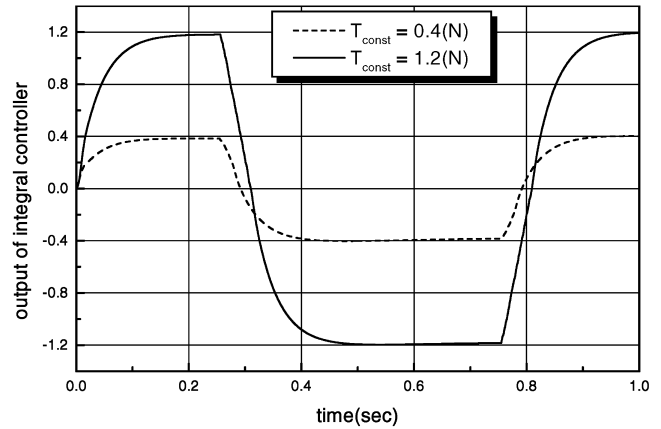


Fig. 2. Output of integral controller with varying Coulomb friction magnitude.

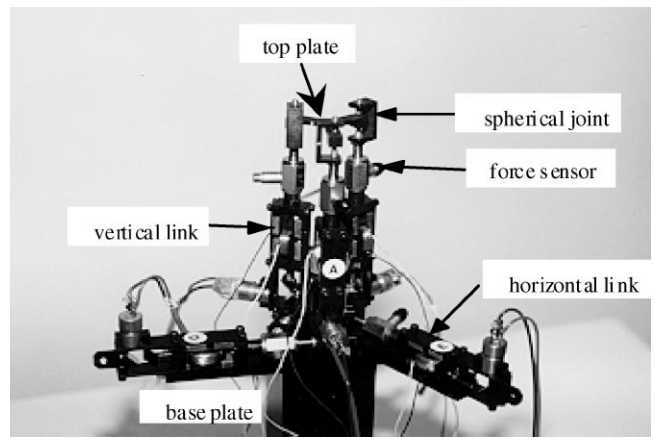


Fig. 3. A photograph of the developed parallel manipulator.

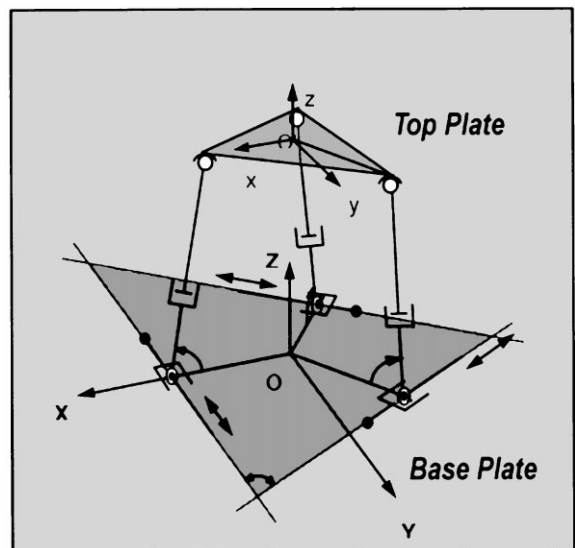


Fig. 4. A kinematic structure of the developed parallel manipulator.

In Eqs. (17) and (18), the steady-state error and integrator output of position command and disturbance is obtained. Table 1 shows this result.

If the desired position command $x_d(s)$ is a step or a sinusoidal function and disturbance $T_l(s)$ has the constant value (T_{const}), the steady-state error becomes zero. However, the integrator output reaches a constant value T_{const}/K_t at the steady state. If the system bandwidth is high enough compared to the desired command frequency range and the Coulomb friction disturbance whose magnitude is δ , the integrator output at steady state just before the sign change of velocity is as follows:

$$u_{I_{ss}} = su_I(s)|_{s=0} = \frac{\delta}{K_t}. \tag{19}$$

Eq. (19) means that the integrator output at the steady state reveals the magnitude of Coulomb friction. Fig. 2 shows the integrator output, which is multiplied by K_t when the desired position command is a 1 Hz sine function. Coulomb friction is regarded as a disturbance and the simulation is performed on two different cases where its magnitudes are 0.4 and 1.2 N, respectively. In Fig. 2, it is shown that the value of the above constant multiplied integrator output is matched to the magnitude of Coulomb friction.

The above result confirms that the integrator output is the estimated value of the friction magnitude divided by the torque constant K_t at the steady state before the velocity sign changes. Therefore, once the integrator output is feed-forwarded by changing the sign at the moment when the velocity sign changes, friction can be

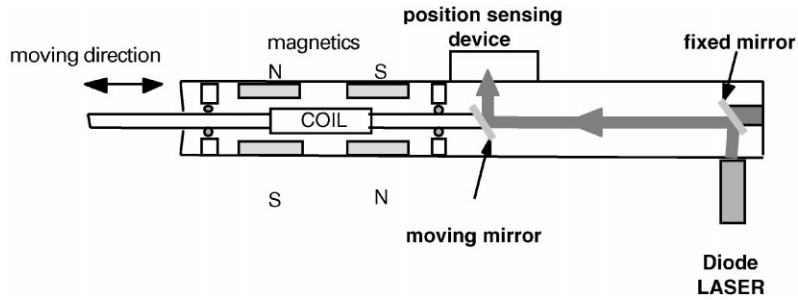


Fig. 5. The joint actuator with an optical sensor.

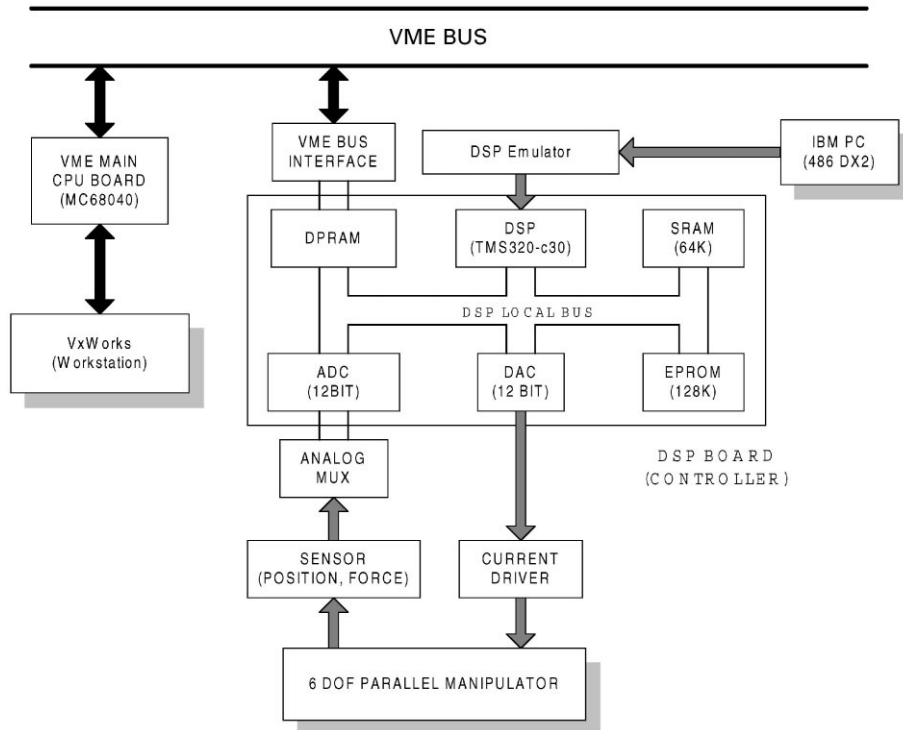


Fig. 6. The experimental system.

compensated for. In other words, the integrator estimates the magnitude of friction by the time that the sign of velocity changes. By reversing the sign of the integrator, the friction is compensated for with the integrator output and the integral controller restarts from the instant that the sign of velocity changes.

Note that if the manipulator has other constant disturbances besides friction, the integrator output may not indicate the exact magnitude of the friction. However, this information can be used to compensate for all the constant disturbances of the manipulator because the integrator output indicates the summed magnitude of all the constant disturbances including the friction.

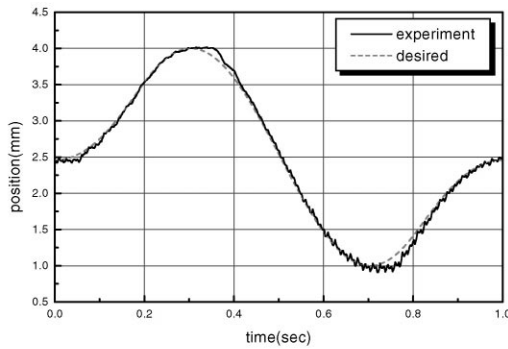
5. Link mechanism of the parallel manipulator

The developed in-parallel 3 PRPS manipulator (Shim, Cho & Kim, 1996; Shim, Park, Kwon, Cho & Kim, 1997) consists of a base plate, a top plate, three actuating horizontal links, and three vertical actuating links as

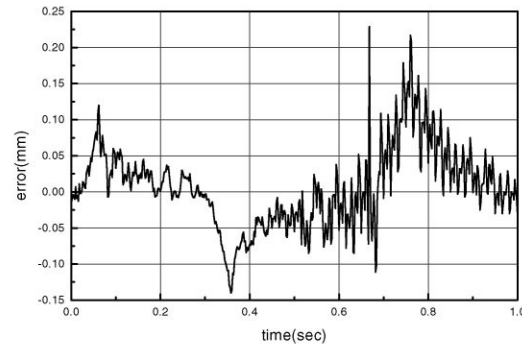
shown in Fig. 3. The three horizontal links provide three degrees-of-freedom, one degree-of-orientation and two degrees-of-translation. The three vertical links provide three degrees-of-freedom, two degrees-of-orientation and one degree-of-translation. The mechanism has been designed as a robot's wrist for micro positioning. The kinematic structures of the parallel manipulator are presented in Fig. 4.

Each joint actuator utilizes the Lorentz force: the force generated by a current-carrying conductor in a static magnetic field as shown in Fig. 4. The position of each actuator is measured by an optical sensor. This sensor is composed of a diode laser, two mirrors and a position-sensing device (PSD). The position sensing resolution of this device is approximately $\pm 5 \mu\text{m}$.

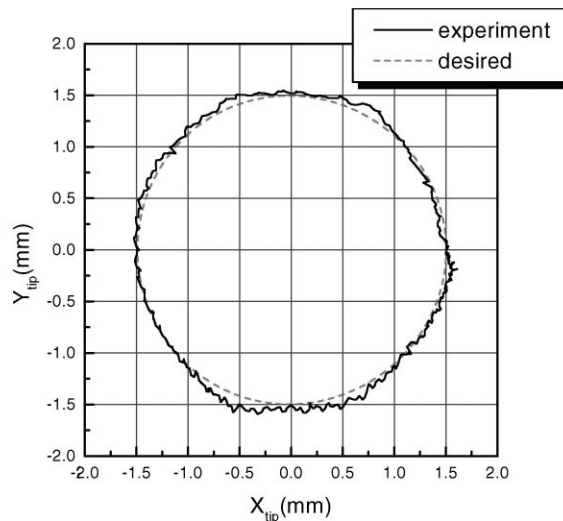
As shown in Fig. 5, a moving coil with the conductor is positioned among the four rectangular neodymium iron boron magnets that provide a high gap field. The coil current I , interacts with the field to produce a pushing force. The force constant measured in the direction of the nominal position is 0.8 N/A and is a torque constant.



(a) trajectory of first link



(b) position error of first link



(c) circular motion of end-effector

Fig. 7. Experiment: circular motion with the PID controller.

6. Experimental results

The experimental setup is shown in Fig. 6. The system consists of a parallel manipulator, a current amplifier, a VME (MC68040) system with a VxWork operation system for trajectory generation, and a DSP (TMS320C30) system for motion control of the manipulator. The main control algorithm is implemented with 1 ms sampling time via the DSP system. The customized DSP system interfaces with the current servo amplifiers and sensors. For a circular motion, the VME system calculates the circular motion, solving kinematics and inverse-kinematics of the parallel manipulator at every 8 ms sampling time. Every 8 ms motion data is transferred to the DSP system through dual-port RAM (DPRAM) and the fine interpolation is implemented via the DSP system to generate each joint position command.

Even though the moving coils of the actuators are expected to be magnetically levitated, the horizontal link motion is not satisfactory due to the friction caused by vertical gravity forces at the sliding bearing. To investigate the effect of nonlinear friction in the circular motion,

a conventional PID control servo system is implemented as shown in Fig. 1. The parameters of the PID controller are selected as

$$K_P = 7, K_I = 0.5 \quad \text{and} \quad K_D = 4,$$

and the system parameters are as:

m is the mass of the moving coil : 0.044 (Kg), K_t is Torque constant : 0.8 (N/A).

The damping coefficient b is ignored. Fig. 7 shows the tracking performance of the PID control by drawing a circle with a radius of 1.5 mm, which represents the first joint tracking performance for this case. It is evident that stiction at three horizontal link actuators affects the tracking performance of the PID control. The PID controller cannot compensate for the error due to the stiction around the near-zero velocity region. The maximum radial tracking error is around 0.223 mm and the *rms* error is 0.0646 mm. Note that there exist rather big peaks at every 60° period due to stiction.

Fig. 8 shows the tracking performance of this proposed method. The maximum radial tracking error is around 0.0780 mm and the *rms* error is 0.0255 mm. This result

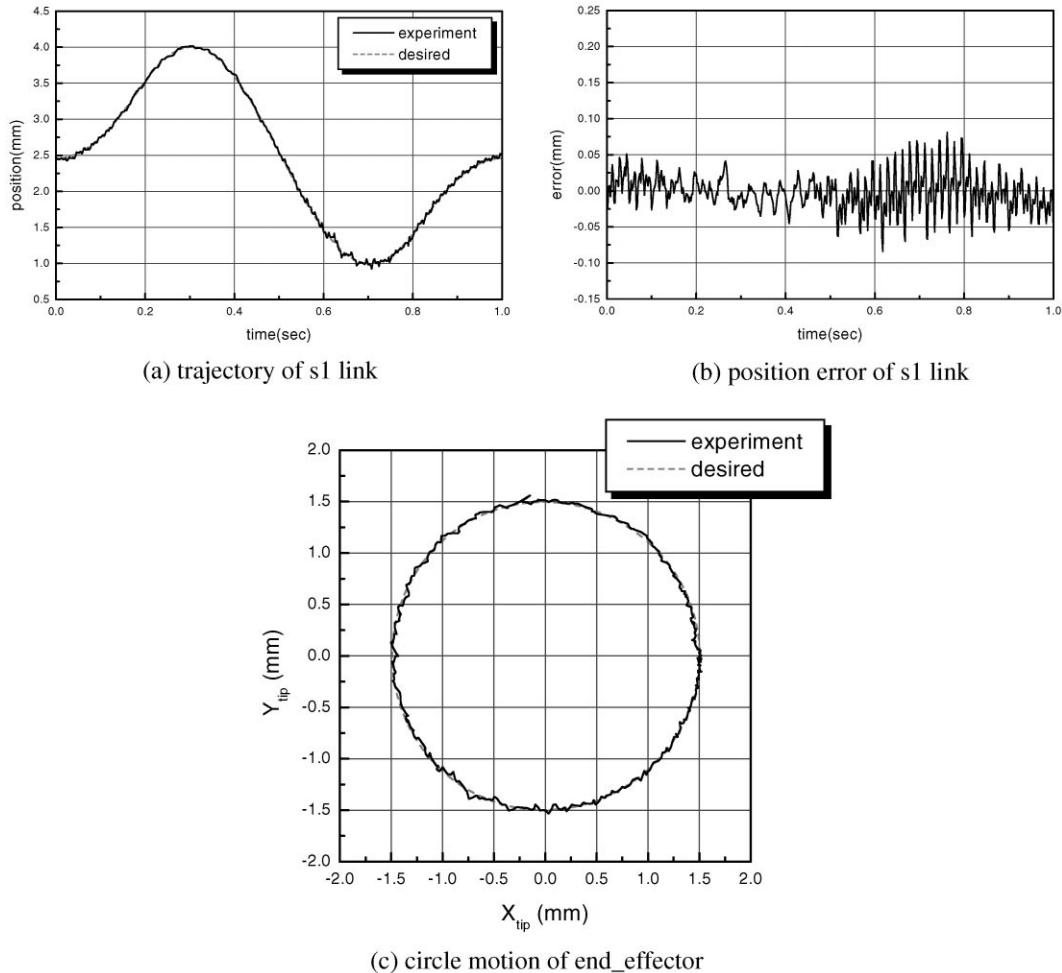


Fig. 8. Experiment: circle motion with the reversed integrator controller.

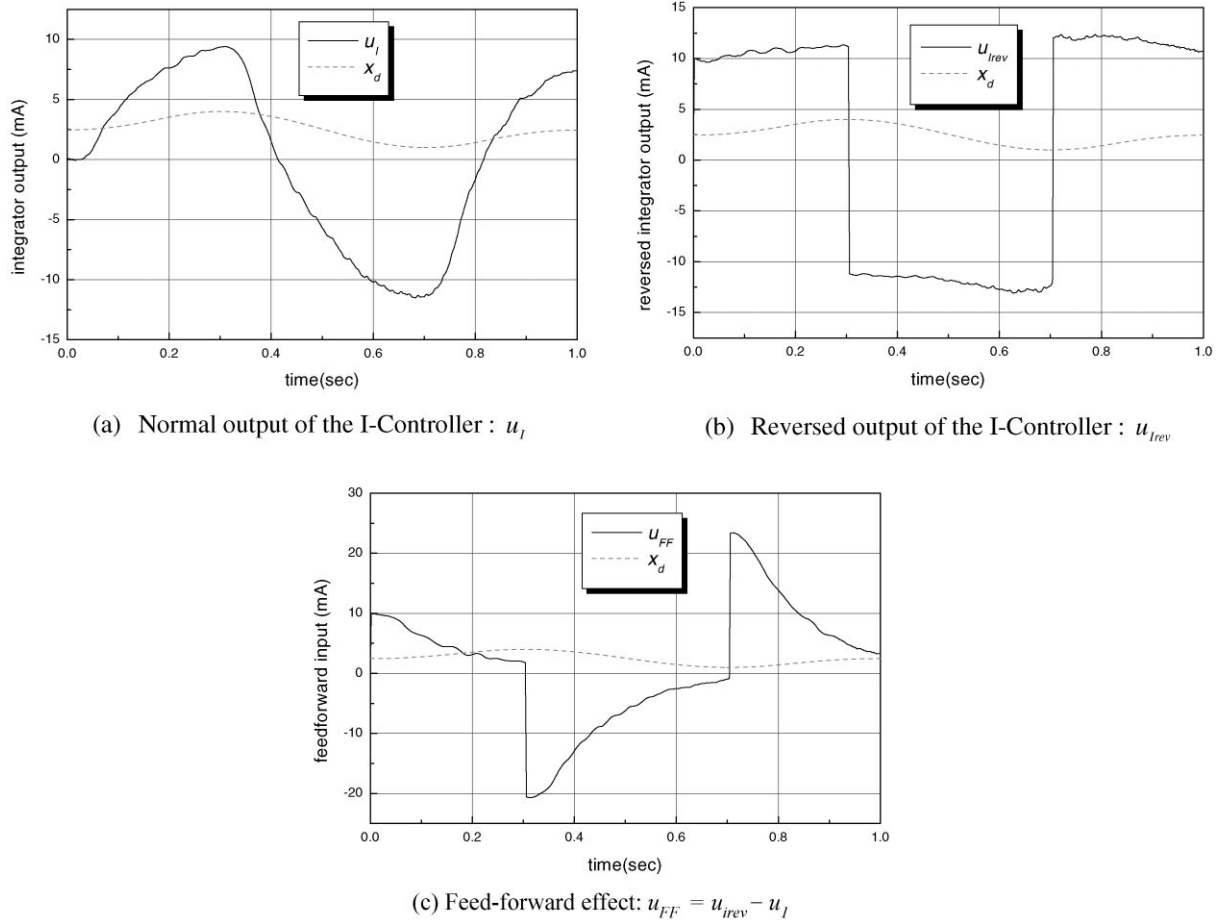


Fig. 9. Integral controller output and its feed-forward effect.

shows a significant improvement compared with the conventional PID controller. This method is very simple but effective in compensating for stiction.

Figs. 9(a) and (b) compare the integrator output of the conventional PID controller and the reversed integrator output of the proposed method, described in Section 3. The dashed line corresponds to the position command for the first link and the solid line corresponds to the integrator output. The sign of the conventional integrator output does not change immediately due to the accumulated errors caused by stiction as shown in Fig. 9(a). Thus, the integrator output degrades the tracking performance. On the other hand, the proposed method reverses the sign of the integrator output as the sign of the velocity of position command changes as shown in Fig. 9(b). Since the actual velocity signal is noisy, catching the instant when the velocity sign changes is difficult in practice. Thus, the integrator output is reversed when the sign of the velocity of position command changes. If the PD gain is large enough to maintain negligible position error, this strategy has been shown to be reasonably effective.

Actually, the reversed integrator output contains the normal integrator output and a feed-forward input. Fig. 9(c) shows the feed-forward input, which is obtained by substituting Fig. 9(a) from Fig. 9(b) as mentioned in (16). This feed-forward input can compensate for friction by reversing the sign of the integrator output immediately at the moment when the sign of the command velocity changes.

7. Conclusion

In this paper, a simple but very effective nonlinear friction compensation method is proposed. The adaptive control strategy is used to explain why the reversed integral-controller effectively compensates for friction of an unknown magnitude. This adaptive scheme is equivalent to reversing the sign of the integrator output as the sign of velocity changes. The integrator output means the estimated magnitude of friction. By reversing the sign of the integrator output immediately at the instant when the sign of velocity changes, the friction is compensated for.

The effectiveness of this proposed approach is demonstrated by experiments on a 3-PRPS (Prismatic-Revolute-Prismatic-Spherical joints) in-parallel 6-DOF manipulator.

The proposed nonlinear friction compensation method is believed to be very useful in the industrial field because it can be realized by a slight modification of the conventional industrial PID controller, whether it is digital or analog.

References

- Armstrong-Helouvy, B. (1993). Stick slip and control in low-speed motion. *IEEE Transactions on Automatic Control*, 38(10), 1483–1496.
- Armstrong-Helouvy, B., Dupont, P. E., & Canudas de Wit, C. (1994). A survey of analysis tools and compensation methods for control of machines with friction. *Automatica*, 30(7), 1083–1138.
- Cai, L., & Song, G. (1993). A smooth robust nonlinear controller for robot manipulators with joint job stick-slip friction. *Proceedings of the IEEE international conference on robotics and automation*, Atlanta, Georgia, USA (pp. 449–454).
- Cai, L., & Song, G. (1994). Joint stick-slip friction compensation of robot manipulators by using smooth robust controller. *Journal of Robotic System*, 11(6), 451–470.
- Canudas de Wit, C., Astrom, K. J., & Braun, K. (1987). Adaptive friction compensation in DC-motor drives. *IEEE International Journal of Robotics and Automation*, 3(6), 681–685.
- Canudas de Wit, C., Astrom, K. J., & Lischinsky, P. (1995). A new model for control of systems with friction. *IEEE Transactions on Automatic Control*, 40(3), 419–425.
- Canudas de Wit, C., & Ge, S. S. (1997). Adaptive friction compensation for systems with generalized velocity/position friction dependency. *Proceedings of the IEEE international conference on decision & control*, San Diego, California, USA (pp. 2465–2470).
- Canudas de Wit, C., Noel, P., Auban, A., & Broglianto, B. (1991). Adaptive friction compensation in robot manipulators: Low velocities. *The International Journal of Robotics Research*, 10(3), 189–199.
- Canudas de Wit, C., Olsson, H., Astrom, K. J., & Lischinsky, P. (1993). Dynamic friction models and control design. *Proceedings of the American Control Conference*, San Francisco, California, USA (pp. 10–12).
- Ge, S. S., Lee, T. H., & Harris, C. J. (1998). *Adaptive neural network control of robotics manipulators*. London: World Scientific.
- Lewis, F. L., Jagannathan, S., & Yesildirek, A. (1998). *Neural network control of robotic manipulators and nonlinear systems*. London: Taylor & Francis.
- Ohnishi, K., Matsui, N., & Hori, Y. (1994). Estimation, identification, and sensorless control in motion control system. *Proceedings of the IEEE*, 82(8), 1253–1265.
- Ohnishi, K., Shiata, M., & Murakami, T. (1996). Motion control for advanced mechatronics. *IEEE/ASME Transactions on Mechatronics*, 1(1), 56–67.
- Polycarpou, M. M., & Ioannou, P. A. (1993). A robust adaptive nonlinear control design. *Proceedings of the American control conference*, San Francisco, California, USA (pp. 1365–1369).
- Radcliffe, C., & Southward, S. (1990). A property of stick-slip friction models which promotes limit cycle generation. *Proceedings of the American control conference*, San Diego, California, USA (pp. 1198–1203).
- Shim, J. H., Cho, H. S., & Kim, S. (1996). A new probing system for the in-circuit test of a PCB. *Proceedings of the IEEE international conference on robotics and automation*, Minneapolis, Minnesota, USA (pp. 580–585).
- Shim, J. H., Park, J. Y., Kwon, D. S., Cho, H. S., & Kim, S. (1997). Kinematic design of a six degree-of-freedom in-parallel manipulator for probing task. *Proceedings of the IEEE international conference on robotics and automation*, Albuquerque, New Mexico (pp. 2967–2973).
- Slotine, J. J. E., & Li, W. (1987). On the adaptive control of robot manipulators. *International Journal of Robotics Research*, 6, 49–57.
- Slotine, J. J. E., & Li, W. (1991). *Applied nonlinear control*. New York: Prentice-Hall.
- Song, J. I., Choi, Y. H., Shim, J. H., Kwon, D. S., & Cho, H. S. (1998). Nonlinear friction compensation methods for an in-parallel actuated 6-DOF manipulator. *Proceedings of IEEE international conference on robotics and automation*, Leuven, Belgium (pp. 169–174).
- Townsend, W., & Salisbury, J. K. (1987). The effect of coulomb friction and stiction on force control. *Proceedings of IEEE international conference on robotics and automation*, Raleigh, North Carolina, USA (pp. 883–889).
- Umeno, T., & Hori, Y. (1991). Robust speed control of DC servomotors using modern two degrees-of-freedom controller design. *IEEE Transactions on Industrial Electronics*, 38(5), 363–368.
- Wu, C. H., & Paul, P. (1980). Manipulator compliance based on joint torque control. *Proceedings of 9th IEEE conference on decision and control*, Albuquerque, NM, USA (pp. 88–94).